ELSEVIER

www.elsevier.nl/locate/jorganchem

Journal of Organometallic Chemistry 593–594 (2000) 465–478

Journal of Organometallic Chemistry

Reactions of binuclear ruthenium–platinum μ-allenyl complexes with nucleophilic and electrophilic reagents. The characterization of two 1:1 adducts of $L(PPh_3)Pt(\mu\text{-}\eta^1{:}\eta^2_{\alpha,\beta}\text{-}C(Ph){=}C{=}CH_2)Ru(CO)Cp$ ($L = PPh_3$, *t*-BuNC) and *p*-toluenesulfonyl isocyanate

Richard R. Willis [a], Mario Calligaris [b,1], Paolo Faleschini [b], Judith C. Gallucci[1] [a], Andrew Wojcicki [a,*]

[a] *Department of Chemistry, The Ohio State University, Columbus, OH 43210, USA*
[b] *Dipartimento di Scienze Chimiche, Universitetá di Trieste, 34127 Trieste, Italy*

Received 2 September 1999; accepted 11 October 1999

Dedicated to Professor Fausto Calderazzo on the occasion of his 70th birthday.

Abstract

Reactions of $(PPh_3)_2Pt(\mu\text{-}\eta^1{:}\eta^2_{\alpha,\beta}\text{-}C(R){=}C{=}CH_2)Ru(CO)Cp$ (R = H (**1**), Ph (**2**)) with $Ph_2PCH_2CH_2CH_2PPh_2$, PEt_3 and *t*-BuNC in THF at −78°C to room temperature afforded the substitution products $L_2Pt(\mu\text{-}\eta^1{:}\eta^2_{\alpha,\beta}\text{-}C(R){=}C{=}CH_2)Ru(CO)Cp$ (R = H, $L_2 = Ph_2PCH_2CH_2CH_2PPh_2$ (**3**), R = Ph, $L_2 = Ph_2PCH_2CH_2CH_2PPh_2$ (**4**), R = H, $L_2 = 2PEt_3$ (**5**), R = Ph, $L_2 = PPh_3$ and *t*-BuNC (**6**)). No reaction was observed for **1** with Et_2NH or $C_6H_{11}NH_2$ and **2** with *p*-$TolS(O)_2NH_2$ in THF at reflux temperature. Complex **2** reacted with *p*-$TolS(O)_2NCO$ (TSI) in toluene at −78°C to room temperature to yield two 1:1 addition products of the reactants: the γ-carbon substituted μ-allenyl $(PPh_3)_2Pt(\mu\text{-}\eta^1{:}\eta^2_{\alpha,\beta}\text{-}C(Ph){=}C{=}CHC(O)NHS(O)_2Tol\text{-}p)$ (**7**) and the [3 + 2] cycloadduct $(PPh_3)_2Pt(\mu\text{-}\eta^1{:}\eta^2\text{-}C{=}C(Ph)N(S(O)_2Tol\text{-}p)C(O)CH_2)Ru(CO)Cp$ (**8**). Complexes **4** and **6** afforded with TSI, under essentially similar conditions, only [3 + 2] cycloadducts, $L_2Pt(\mu\text{-}\eta^1{:}\eta^2\text{-}C{=}C(Ph)N(S(O)_2Tol\text{-}p)C(O)CH_2)Ru(CO)Cp$ ($L_2 = Ph_2PCH_2CH_2CH_2PPh_2$ (**9**), PPh_3 and *t*-BuNC (**10**)). All products were characterized by a combination of IR and NMR (^1H, $^{13}C\{^1H\}$ and $^{31}P\{^1H\}$) spectroscopy, FAB MS and elemental analysis. The structures of **7** (as **7**·C_3H_6O) and **10** were determined by single-crystal X-ray diffraction analysis. Reactions of **2** with *trans*-NCCH=CHCN (L) and of **1** with the alkynes $MeO_2CC{\equiv}CCO_2Me$, $MeO_2CC{\equiv}CMe$, $PhC{\equiv}CH$ and $PhC{\equiv}CPh$ (L) resulted in the formation of the mononuclear metal complexes $Cp(CO)_2RuC(R){=}C{=}CH_2$ (R = H, Ph) and $(PPh_3)_2PtL$. The reverse of this fragmentation reaction occurred when $Cp(CO)_2RuCH{=}C{=}CH_2$ was treated with $(PPh_3)_2Pt(PhC{\equiv}CPh)$. No reaction was observed between **2** and each $(CN)_2C{=}CPh_2$ and $MeS(O)_2NSO$ in benzene or toluene on heating. The η^1-allenyl $Cp(CO)_2RuC(Ph){=}C{=}CH_2$, obtained in this study, is a new compound. © 2000 Elsevier Science S.A. All rights reserved.

Keywords: Mixed-metal complexes; Platinum; Ruthenium; $\mu\text{-}\eta^1{:}\eta^2_{\alpha,\beta}$-Allenyl; Cycloaddition; X-ray structures

1. Introduction

Reaction chemistry of binuclear and trinuclear transition-metal μ-allenyl complexes is an expanding area of research activity [1–3]. In particular, homobinuclear $\mu\text{-}\eta^1{:}\eta^2$-allenyl complexes of the general formula $(CO)_3M(\mu\text{-}PPh_2)(\mu\text{-}\eta^1{:}\eta^2\text{-allenyl})M(CO)_3$ (M = Fe or Ru) have received recent attention [3–9]. Reactions of these complexes with a variety of nucleophilic reagents have been found to proceed by addition of the latter to the μ-allenyl fragment, to one of the carbonyl ligands or to the metal.

* Corresponding author.
E-mail address: wojcicki.1@osu.edu (A. Wojcicki)

[1] Inquiries concerning X-ray crystallographic studies should be addressed to M.C. (**7**·C_3H_6O) and J.C.G. (**10**).

0022-328X/00/$ - see front matter
PII: S0022-328X(99)00613-0

We have recently reported [10] that the complexes $(PPh_3)_2Pt(\mu\text{-}\eta^1{:}\eta^2_{\alpha,\beta}\text{-}C(R){=}C{=}CH_2)Ru(CO)Cp$(R = H (**1**), Ph (**2**)) react with the electrophilic species $(PPh_3)Au^+$ to afford trimetallic η^3-allyl complexes, $[(PPh_3)_2Pt(\mu_2\text{-}CO)RuCpAu(PPh_3)(\mu_3\text{-}\eta^1{:}\eta^3{:}\eta^1\text{-}CH_2\text{-}CCR)]^+$ (Eq. (1)).

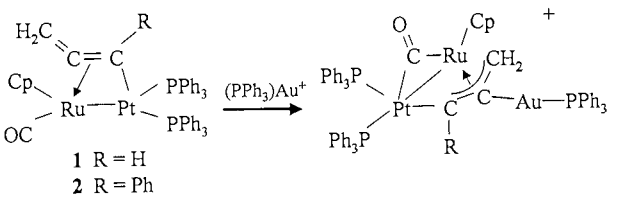

(1)

The present paper is concerned with reactions of **1**, **2** and related ruthenium–platinum binuclear $\mu\text{-}\eta^1{:}\eta^2_{\alpha,\beta}$-allenyl complexes with other electrophilic reagents, as well as with some nucleophilic reagents. The chemistry is highlighted by [3 + 2] cycloaddition of *p*-toluenesulfonyl isocyanate to the μ-allenyl ligand and by fragmentation of **1** and **2** into mononuclear ruthenium η^1-allenyl and $(PPh_3)_2Pt$(alkene or alkyne) complexes upon reaction with alkenes and alkynes.

2. Experimental

2.1. General procedures

All reactions and manipulations were conducted under an atmosphere of Ar using standard procedures [11]. Solvents were dried, distilled under an Ar atmosphere and degassed before use [12]. Elemental analyses were performed by M-H-W Laboratories, Phoenix, AZ. Melting points were measured on a Thomas–Hoover melting point apparatus and are uncorrected. ^{1}H-, ^{13}C- and ^{31}P-NMR spectra were recorded on a Bruker AM-300 spectrometer, and IR spectra were obtained on a Perkin–Elmer model 283B spectrophotometer. Mass spectra (FAB) were recorded on a Kratos VG70-250S spectrometer by Mr David C. Chang.

Reagents were obtained from various commercial sources and used as received with the exception of TCNE, which was sublimed, and *p*-TolS(O)$_2$NCO and $C_6H_{11}NH_2$, which were distilled, the former from P_4O_{10}. Literature procedures were followed to synthesize MeS(O)$_2$NSO [13], $(PPh_3)_2Pt(C_2H_4)$ [14], $(PPh_3)_2Pt(PhC{\equiv}CPh)$ [15], $Cp(CO)_2RuCH{=}C{=}CH_2$ [16], and $(PPh_3)_2Pt(\mu\text{-}\eta^1{:}\eta^2_{\alpha,\beta}\text{-}C(R){=}C{=}CH_2)Ru(CO)Cp$ (R = H, Ph) [17].

2.2. Reactions of $(PPh_3)_2Pt(\mu\text{-}\eta^1{:}\eta^2_{\alpha,\beta}\text{-}C(R){=}C{=}CH_2)$-Ru(CO)Cp (R = H (**1**), Ph (**2**)) with nucleophilic reagents

2.2.1. Reaction of **1** with $Ph_2PCH_2CH_2CH_2PPh_2$

To a stirred solution of **1** (0.28 g, 0.29 mmol) in THF (15 ml) at −78°C was added dropwise over 3 min a THF solution (5 ml) of $Ph_2PCH_2CH_2CH_2PPh_2$ (0.12 g, 0.29 mmol). The resulting solution was allowed to warm to room temperature (r.t.) over 6 h, and solvent was removed under reduced pressure. The residue was dissolved in THF (3 ml), treated with hexane (7 ml), and cooled at ca. −10°C for 18 h. The yellow precipitate of $(Ph_2PCH_2CH_2CH_2PPh_2)Pt(\mu\text{-}\eta^1{:}\eta^2_{\alpha,\beta}\text{-}CH{=}C{=}CH_2)Ru(CO)Cp$ (**3**) was collected on a frit. Yield, 0.12 g (49%). M.p. 165°C dec. Selected data for **3**: IR (MeCN): ν(CO) 1902 (s), ν(C=C=C) 1714 (m) cm^{-1}. ^{1}H-NMR ($CDCl_3$): δ 7.7–7.0 (m, 20H, Ph), 6.70 (s, br, J_{PtH} = 37 Hz, 1H, =CH), 5.59 (s, br, J_{PtH} = 27 Hz, 1H of =CH$_2$), 4.77 (s, br, J_{PtH} = 18 Hz, 1H of =CH$_2$), 4.58 (s, 5H, Cp). ^{13}C{^{1}H}-NMR (CD_2Cl_2): δ 206.5 (s, CO), 168.9 (s, =C=), 112.4 (d, J_{PC} = 85 Hz, J_{PtC} = 722 Hz, =CH), 94.5 (s, =CH$_2$), 82.3 (s, Cp), 27.2, 20.6 (2s, CH$_2$). ^{31}P{^{1}H} (CD_2Cl_2): δ 5.4 (d, J_{PP} = 20 Hz, J_{PtP} = 2564 Hz), 1.5 (d, J_{PP} = 20 Hz, J_{PtP} = 3406 Hz). FAB MS: ^{102}Ru, ^{195}Pt, *m*/*z* (ion, relative intensity) 841 (M^+, 19.2), 813 (M^+–CO, 3.7), ($Pt(Ph_2P(CH_2)_3PPh_2)^+$, 10.3). Anal. Found: C, 51.66; H, 4.26. $C_{36}H_{34}OP_2PtRu$. Calc.: C, 51.43; H, 4.08.

2.2.2. Reaction of **2** with $Ph_2PCH_2CH_2CH_2PPh_2$

A stirred solution of **2** (0.22 g, 0.21 mmol) in THF (15 ml) at −78°C was treated dropwise over 10 min with a solution of $Ph_2PCH_2CH_2CH_2PPh_2$ (0.068 g, 0.21 mmol) in THF (5 ml). The resulting solution was allowed to warm to r.t. over 6 h and was stirred for an additional 18 h. The solvent was removed under reduced pressure, the residue was dissolved in THF (2 ml), and hexane (7 ml) was added with stirring. Cooling at ca. −10°C for 18 h produced a yellow precipitate of $(Ph_2PCH_2CH_2CH_2PPh_2)Pt(\mu\text{-}\eta^1{:}\eta^2_{\alpha,\beta}\text{-}C(Ph){=}C{=}CH_2)$-Ru(CO)Cp (**4**), which was collected by filtration. Yield, 0.077 g (40%). Selected data for **4**: IR (CH_2Cl_2): ν(CO) 1901 (s), ν(C=C=C) 1712 (m) cm^{-1}. ^{1}H-NMR (C_6D_6): δ 7.7–7.1 (m, 25H, Ph), 6.12 (d, J_{HH} = 2.2 Hz, J_{PtH} = 24 Hz, 1H of =CH$_2$), 5.56 (d, J_{HH} = 2.2 Hz, J_{PtH} = 15 Hz, 1H of =CH$_2$), 4.46 (s, 5H, Cp). ^{31}P{^{1}H}-NMR (C_6D_6): δ 4.0 (d, J_{PP} = 22.5 Hz, J_{PtP} = 2526 Hz), −1.1 (d, J_{PP} = 22.5 Hz, J_{PtP} = 3427 Hz). FAB MS: ^{102}Ru, ^{195}Pt, *m*/*z* (ion, relative intensity) 918 (M^+ + 1, 31.3), 890 (M^+ + 1-CO, 3.7), 607 ($Pt(Ph_2P(CH_2)_3PPh_2)^+$, 9.2).

2.2.3. Reaction of **1** with PEt_3

A stirred solution of **1** (0.10 g, 0.11 mmol) in THF (20 ml) at −78°C was treated dropwise with PEt_3 (0.050 ml, 0.34 mmol). The resulting solution was then allowed to warm to r.t. over 6 h, and the solvent was freed under vacuum. THF (2 ml) was added to the residue and the orange solution/suspended white solid was passed through a layer of Celite, which was washed with additional (8 ml) THF. The filtrate was concentrated to 2 ml and hexane (10 ml) was carefully layered on top of the orange THF solution. After slow diffu-

sion of the two solvents at 0°C for 24 h, a yellow solid of $(PEt_3)_2Pt(\mu\text{-}\eta^1{:}\eta^2_{\alpha,\beta}\text{-}CH{=}C{=}CH_2)Ru(CO)Cp$ (**5**) was isolated by filtration. Yield, 0.062 g (85%). Selected data for **5**: IR (CH_2Cl_2): ν(CO) 1892 (s) cm^{-1}. ^{1}H-NMR ($CDCl_3$): δ 6.42 (m, $J_{PtH} = 31$ Hz, 1H, =CH), 5.41 (m, $J_{PtH} = 20$ Hz, 1H of $=CH_2$), 5.00 (s, 5H, Cp), 4.70 (m, $J_{PtH} = 13$ Hz, 1H of $=CH_2$), 2.1–0.75 (several m, 30H, Et). $^{31}P\{^1H\}$-NMR ($CDCl_3$): δ 23.9 (s, br, $J_{PtP} = 3681$ Hz), 12.4 (s, br, $J_{PtP} = 2733$ Hz). FAB MS: ^{102}Ru, ^{195}Pt, m/z (ion, relative intensity) 665 (M^+, 6.1), 547 ($M^+ - PEt_3$, 6.0), 429 ($M^+ - 2PEt_3$, 12.1).

2.2.4. Reaction of 2 with t-BuNC

A stirred orange–red solution of **2** (0.20 g, 0.19 mmol) in THF (10 ml) at −78°C was treated dropwise over 5 min with *t*-BuNC (0.10 ml, 0.89 mmol). The color of the solution immediately turned yellow although the reaction was not complete at this point, as ascertained by NMR spectroscopy. The solution was allowed to warm to r.t. over 8 h and was stirred for an additional 8 h. The solvent was removed under reduced pressure and the yellow residue was treated with 5 ml of 4:1 hexane–THF. Filtration afforded (0.12 g, 67% yield) $(t\text{-BuNC})(PPh_3)Pt(\mu\text{-}\eta^1{:}\eta^2_{\alpha,\beta}\text{-}C(Ph){=}C{=}CH_2)Ru(CO)Cp$ (**6**) as a yellow solid. M.p. 98°C. Selected data for **6**: IR (CH_2Cl_2): 1901 (s) cm^{-1}. ^{1}H-NMR ($CDCl_3$): δ 7.8–6.7 (m, 20H, Ph), 5.62 (s, $J_{PtH} = 17$ Hz, 1H of $=CH_2$), 4.98 (s, $J_{PtH} = 13$ Hz, 1H of $=CH_2$), 4.74 (s, 5H, Cp), 1.29 (s, 9H, Me). $^{13}C\{^1H\}$-NMR (CD_2Cl_2): δ 205.0 (s, $J_{PtC} = 50.4$ Hz, CO), 166.5 (s, =C=), 150.1 (s, =*C*Ph), 143.8 (s, br, CN?), 97.0 (s, $J_{PtC} = 32.2$ Hz, $=CH_2$), 84.1 (s, Cp), 57.0 (s, C of *t*-Bu), 29.9 (s, Me). $^{31}P\{^1H\}$-NMR ($CDCl_3$): δ 25.6 (s, $J_{PtP} = 3544$ Hz). FAB MS: ^{102}Ru, ^{195}Pt, m/z (ion, relative intensity) 850 (M^+, 68.0), 767 (M^+–BuNC, 9.4). Anal. Found: C, 54.01; H, 4.51. $C_{38}H_{36}NOPPtRu$ Calc.: C, 53.71; H, 4.27.

2.2.5. Reactions of 1 and 2 with nitrogen nucleophiles

In a typical experiment, a solution of **1** (0.20 g, 0.21 mmol) and Et_2NH (0.050 ml, 0.49 mmol) in THF (30 ml) first at r.t. and then at reflux temperature was monitored by ^{1}H- and ^{31}P-NMR spectroscopy. No changes were noted over 1 h of reaction time. Similar results were obtained for reactions of **1** with $C_6H_{11}NH_2$ and **2** with $p\text{-TolS(O)}_2NH_2$.

2.3. Reactions of $L_2Pt(\mu\text{-}\eta^1{:}\eta^2_{\alpha,\beta}\text{-}C(Ph){=}C{=}CH_2)Ru(CO)Cp$ ($L_2 = 2PPh_3$ (**2**), $Ph_2PCH_2CH_2CH_2PPh_2$ (**4**), PPh_3 and *t*-BuNC (**6**)) with $p\text{-TolS(O)}_2NCO$ (TSI)

2.3.1. Reaction of 2 with TSI

A stirred solution of **2** (0.15 g, 0.15 mmol) in toluene (7 ml) at −78°C was treated with 3.0 ml of a 0.079 M solution of TSI (0.24 mmol) in toluene. The resulting red solution was allowed to warm to r.t. over 8 h and was stirred for an additional 10 h. A yellow solid of $(PPh_3)_2Pt(\mu\text{-}\eta^1{:}\eta^2_{\alpha,\beta}\text{-}C(Ph){=}C{=}CHC(O)NHS(O)_2Tol\text{-}p)Ru(CO)Cp$ (**7**) was then separated from an orange solution by filtration. Yield, 0.10 g (54%). Selected data for **7**: IR (CH_2Cl_2): ν(CO) 1924 (s), 1670 (s) cm^{-1}. ^{1}H-NMR ($CDCl_3$): δ 12.1 (s, 1H, NH), 8.1–6.8 (m, 39H, Ph and C_6H_4), 5.96 (s, $J_{PtH} = 10$ Hz, 1H, =CH), 4.48 (s, 5H, Cp), 2.43 (s, 3H, Me). $^{13}C\{^1H\}$-NMR ($CDCl_3$): δ 201.9 (s, RuCO), 178.1 (s, NCO), 164.5 (s, =C=), 146.2 (s, =*C*Ph), 108.4 (s, =CH), 86.6 (s, Cp), 21.5 (s, Me). $^{31}P\{^1H\}$-NMR ($CDCl_3$): δ 21.6 (d, $J_{PP} = 11$ Hz, $J_{PtP} = 2789$ Hz), 20.9 (d, $J_{PP} = 11$ Hz, $J_{PtP} = 3923$ Hz). FAB MS: ^{102}Ru, ^{195}Pt, m/z (ion, relative intensity) 1226 (M^+, 16.3), 1198 (M^+–CO, 9.8), 964 ($M^+ - PPh_3$, 21.6), 719 ($Pt(PPh_3)_2^+$, 100). Anal. Found: C, 57.64; H, 4.12. $C_{59}H_{49}NO_4P_2PtRuS$ Calc.: C, 57.79; H, 4.03.

The orange filtrate was evaporated to dryness, and the residue was extracted with 3:1 hexane–toluene (3 × 9 ml). The solvent was removed from the combined extracts to leave a small amount (< 0.020 g, < 11% yield) of $(PPh_3)_2Pt(\mu\text{-}\eta^1{:}\eta^2\text{-}C{=}C(Ph)N(S(O)_2Tol\text{-}p)C(O)CH_2)Ru(CO)Cp$ (**8**). Selected data for **8**: IR (CH_2Cl_2): ν(CO) 1899 (s), 1724 (s) cm^{-1}. ^{1}H-NMR (C_6D_6): δ 8.5–6.5 (m, 39H, Ph and C_6H_4), 4.84 (s, 5H, Cp), 3.71 (d, $J_{HH} = 21.3$ Hz, $J_{PtH} = 17.2$ Hz, 1H of CH_2), 2.72 (dt, $J_{HH} = 21.3$ Hz, $J_{PH} = 14.5$ Hz, 1H of CH_2), 1.88 (s, 3H, Me). $^{13}C\{^1H\}$-NMR (C_6D_6): δ 206.2 (s, RuCO), 174.5 (d, $J_{PC} = 8.5$ Hz, $J_{PtC} = 120$ Hz, =*C*Pt), 153.1 (s, =*C*Ph), 151.5 (s, NCO?), 86.3 (s, Cp), 52.5 (s, $J_{PtC} = 54.7$ Hz, CH_2), 20.6 (s, Me). $^{31}P\{^1H\}$-NMR (C_6D_6): δ 22.7 (d, $J_{PP} = 11.3$ Hz, $J_{PtP} = 2643$ Hz), 16.3 (d, $J_{PP} = 11.3$ Hz, $J_{PtP} = 3621$ Hz). FAB MS: ^{102}Ru, ^{195}Pt, m/z (ion, relative intensity) 1226 (M^+, 25.4), 719 ($Pt(PPh_3)_2^+$, 100). Anal. Found: C, 57.88; H, 4.43. $C_{59}H_{49}NO_4P_2PtRuS$ Calc.: C, 57.79; H, 4.03.

2.3.2. Reaction of 4 with TSI

A stirred solution of **4** (0.27 g, 0.29 mmol) in benzene (10 ml) at r.t. was treated with TSI (0.075 ml, 0.49 mmol). After 15 h of stirring, the solvent was removed under vacuum and the orange residue was thoroughly washed with hexane (2 × 15 ml) to yield (0.17 g, 53%) a yellow powder of $(Ph_2PCH_2CH_2CH_2PPh_2)Pt(\mu\text{-}\eta^1{:}\eta^2\text{-}C{=}C(Ph)NS(O)_2Tol\text{-}p)C(O)CH_2)Ru(CO)Cp$ (**9**). Selected data for **9**: IR (CH_2Cl_2) ν(CO) 1894 (s), 1708 (m) cm^{-1}. ^{1}H-NMR ($CDCl_3$): δ 8.0–6.8 (m, 29H, Ph and C_6H_4), 4.55 (s, 5H, Cp), 3.41 (d, $J_{PH} = 23$ Hz, $J_{PtH} = 21$ Hz, 1H of CH_2), 2.82 (m, 1H of CH_2). $^{31}P\{^1H\}$-NMR ($CDCl_3$): δ 0.47 (d, $J_{PP} = 26.5$ Hz, $J_{PtP} = 2362$ Hz), −6.6 (d, $J_{PP} = 26.5$ Hz, $J_{PtP} = 3468$ Hz). FAB MS: ^{102}Ru, ^{195}Pt, m/z (ion, relative intensity) 1114 (M^+, 24.2), 1086 (M^+–CO, 20.3), 607 ($Pt(Ph_2P(CH_2)_3PPh_2)^+$, 61.6).

*2.3.3. Reaction of **6** with TSI*

A stirred solution of **6** (0.10 g, 0.12 mmol) in toluene (7 ml) at −78°C was treated dropwise over 5 min with 3.0 ml of a 0.079 M solution of TSI (0.24 mmol) in toluene. The resulting solution was allowed to warm to r.t. over 6 h and was stirred for an additional 12 h. The volume was reduced to about 1 ml, and hexane (10 ml) was added with vigorous stirring to induce the precipitation of a yellow solid of (t-BuNC)(PPh_3)Pt(μ-η^1:η^2-C=C(Ph)NS(O)$_2$Tol-p)C(O)CH_2)Ru(CO)Cp (**10**). Yield, 0.075 g (60%). Selected data for **10**: IR (CH_2Cl_2) ν(CO) 1908 (s), 1714 (m) cm^{-1}. ^{1}H-NMR (C_6D_6): δ 8.3–6.5 (m, 24H, Ph and C_6H_4), 5.38 (s, 5H, Cp), 3.66 (dd, J_{HH} = 21.6 Hz, J_{PH} = 1.8 Hz, J_{PtH} = 50 Hz, 1H of CH_2), 3.29 (dd, J_{HH} = 21.6 Hz, J_{PH} = 6.6 Hz, 1H of CH_2). ^{13}C{^{1}H}-NMR (C_6D_6): δ 203.1 (s, RuCO), 167.7 (s, =CPt), 141.1 (s, =*C*Ph), 85.3 (s, Cp), 52.7 (s, CH_2), 21.1 (s, Me). ^{31}P{^{1}H}-NMR (C_6D_6): δ 14.6 (s, J_{PtP} = 3538 Hz). FAB MS: ^{102}Ru, ^{195}Pt, m/z (ion, relative intensity) 1047 (M^+, 14.0), 1019 (M^+–CO, 9.3), 850 (M^+–TolSO$_2$NCO, 100). Anal. Found: C, 52.51; H, 4.27. $C_{46}H_{43}N_2O_4PPtRuS$ Calc.: C, 52.77; H, 4.14.

*2.4. Reactions of (PPh_3)$_2$Pt(μ-η^1:η$^2_{\alpha,\beta}$-C(R)=C=CH_2)-Ru(CO)Cp (R = H (**1**), Ph (**2**)) with other unsaturated organic compounds*

*2.4.1. Reactions of **1** with alkynes*

A stirred solution of **1** (0.10–0.20 g, 0.11–0.21 mmol) in THF (5–10 ml) at −78°C or r.t. was treated with 1–2 equivalents of $MeO_2CC{\equiv}CCO_2Me$, $MeO_2CC{\equiv}CMe$, PhC≡CH or PhC≡CPh. The solutions at −78°C were allowed to warm to r.t. and all solutions were stirred at ca. 25°C for 3–12 h. Aliquots were withdrawn, freed of the solvent, and the residue was dissolved in a deuteriated solvent and examined by ^{1}H and/or ^{13}P-NMR spectroscopy.

*2.4.2. Reactions of **2** with $(CN)_2C{=}CPh_2$, trans-NCCH=CHCN and $MeS(O)_2NSO$*

A stirred solution of **2** (0.15–0.20 g, 0.15–0.19 mmol) in benzene or toluene (ca. 10 ml) at r.t. was treated with 1–2 equivalents of $(CN)_2C{=}CPh_2$, *trans*-NCCH=CHCN or $MeS(O)_2NSO$. No reaction was observed by ^{31}P-NMR spectroscopy in 2–6 h. The solution was then maintained at reflux temperature for 2–4 h, cooled, and examined by ^{1}H and/or ^{31}P-NMR spectroscopy as described for the preceding experiments (Section 2.4.1).

*2.4.3. Reactions of **1** with $(CN)_2C{=}C(CN)_2$*

To a stirred solution of **1** (0.20 g, 0.21 mmol) in CH_2Cl_2 (10 ml) at −78°C was added solid $(CN)_2C{=}C(CN)_2$ (0.030 g, 0.23 mmol). After 1 h of reaction time the solution was examined by ^{31}P{^{1}H}-NMR spectroscopy: δ 26.6 (d, J_{PP} = 7.0 Hz, J_{PtP} = 2891 Hz), 19.7 (d, J_{PP} = 7.0 Hz, J_{PtP} = 3248 Hz), 14.5 (s, J_{PtP} = 3748 Hz), among a host of other signals. After the solution was allowed to warm to r.t., the above signals disappeared except for the signal at δ 14.5.

*2.4.4. Reaction of **2** with $ClS(O)_2NCO$*

To a stirred solution of **2** (0.16 g, 0.16 mmol) in THF (10 ml) at −78°C was added dropwise over 1 min $ClS(O)_2NCO$ (0.060 ml, 0.68 mmol). The resulting solution was stirred for 1 h, during which time its color changed from orange to dark red. Warming to r.t. over 6 h and stirring for an additional 12 h yielded a cloudy brown solution. This solution was filtered and the solvent was removed from the filtrate to yield a brown tar. Attempted purification of the tar by crystallization or chromatography resulted in decomposition.

*2.5. Reaction of (PPh_3)$_2$Pt(μ-η^1:η$^2_{\alpha,\beta}$-C(Ph)=C=CH_2)-Ru(CO)Cp (**2**) with CO followed by p-TolS(O)$_2$NCO (TSI)*

Carbon monoxide was bubbled through a solution of **2** (0.10 g, 0.10 mmol) in toluene (10 ml) at r.t. for 18 h to ensure conversion of the latter to Cp(CO)$_2$-RuC(Ph)=C=CH_2 and (PPh_3)$_2$Pt(CO)$_2$. The reaction solution was then placed under an Ar atmosphere, cooled to −78°C, and treated with two equivalents of TSI (0.079 M solution, 0.20 mmol) in toluene (2.5 ml). The resulting solution was allowed to warm to r.t. over 1 h, during which time a white precipitate had formed. A ^{31}P{^{1}H}-NMR spectrum ($CDCl_3$) of the solid showed a singlet resonance at δ 5.10 (J_{PtP} = 3698 Hz). A ^{1}H-NMR spectrum ($CDCl_3$) of the material remaining in solution revealed resonances of Cp(CO)$_2$RuC-(Ph)=C=CH_2 (δ 5.28 (s, 5H, Cp), 4.14 (s, 2H, =CH_2)) and of another Ru compound (δ 5.00 (s, 5H, Cp), 3.16 (s, 2H, CH_2)). The reaction solution was filtered to remove the precipitate, the solvent was removed under reduced pressure from the filtrate and hexane (10 ml) was added to the red residue. After the mixture had been stirred for 18 h, an orange powder was isolated by filtration. FAB MS: ^{102}Ru, m/z (ion, relative intensity) 339 (M^+ + 1, 20.6), 311 (M^+ + 1-CO, 7.8), 283 (M^+ + 1-2CO, 21.9) (M = Cp(CO)$_2$RuC$_3$H$_2$Ph). No satisfactory FAB MS data were obtained for the other Ru compound. Attempts at separation/purification of the orange powder by chromatography on alumina were unsuccessful.

2.6. Crystallographic analyses

*2.6.1. (PPh_3)$_2$Pt(μ-η^1:η$^2_{\alpha,\beta}$-C(Ph)=C=CHC-(O)NHS(O)$_2$Tol-p)Ru(CO)Cp·C_3H_6O (**7**·C_3H_6O)*

Crystals of **7**·C_3H_6O were grown from dichloromethane–acetone. Lattice constants were determined

by a least-squares refinement of 25 reflections, accurately centered on an Enraf–Nonius CAD4 diffractometer. A summary of the crystal data and refinement is presented in Table 1. No significant change in intensities of control reflections was observed over the course of data collection. The data were corrected for Lorentz polarization effects, as well as for absorption, through an empirical correction based on the ψ scans of four close-to-axial reflections [18]. The structure was solved by Patterson and Fourier methods [18] and refined on F^2 by least-squares methods [19]. A difference Fourier map revealed the presence of one acetone molecule disordered over two positions (occupancy factor 50%). Hydrogen atoms were located in calculated positions and refined as riding, including free torsion of the methyl groups. U_{iso} values for H atoms were set to $1.2U_{eq}$ values of the parent carbon or nitrogen atoms. The hydrogen atoms of the solvent molecules were not included in the calculations. Final full-matrix least-squares refinement converged to $R = 0.059$. Anisotropic temperature factors were assigned to all non-hydrogen atoms, with exclusion of the acetone molecules, which were refined isotropically with distance constraints.

Table 1
Crystal data and experimental details for $(PPh_3)_2Pt(\mu\text{-}\eta^1{:}\eta^2_{\alpha,\beta}\text{-}C(Ph)=C=CHC(O)NHS(O)_2Tol\text{-}p)Ru(CO)Cp\cdot C_3H_6O$ (**7**·C_3H_6O) and $(t\text{-}BuNC)(PPh_3)Pt(\mu\text{-}\eta^1{:}\eta^2\text{-}C=C(Ph)N(S(O)_2Tol\text{-}p)C(O)CH_2)Ru(CO)Cp$ (**10**)

	7·C_3H_6O	**10**
Molecular formula	$C_{59}H_{49}NO_4P_2PtRuS\cdot C_3H_6O$	$C_{46}H_{43}N_2O_4PPtRuS$
Formula weight	1284.31	1047.05
Crystal system	Triclinic	Monoclinic
Space group	$P\bar{1}$	$P2_1/n$
a (Å)	10.797(6)	11.502(3)
b (Å)	12.050(10)	16.518(4)
c (Å)	22.809(20)	23.008(5)
α (°)	78.64(5)	
β (°)	89.72(5)	102.50(2)
γ (°)	86.82(5)	
V (Å^3)	2904.8(8)	4268(2)
Z	2	4
$D_{calc.}$ (g cm^{-3})	1.47	1.63
Temperature (°C)	Ambient	23
μ (cm^{-1})	28.2	37.8
Crystal size (mm)	$0.30\times0.33\times0.40$	$0.19\times0.31\times0.31$
Radiation	Mo–K_α, graphite ($\lambda = 0.71073$ Å)	
Scan type	$\omega/2\theta$	ω
Scan angle (°)	$0.60+0.35\tan\theta$ [a]	$1.30+0.35\tan\theta$
2θ range (°)	4–54	4–55
Transmission factors	0.84–1.00	0.71–1.00
No. of unique reflections measured	12638	10155
No. of reflections with $I>2\sigma(I)$	9282	4763
No. of parameters	654	497
Minimized function	$\Sigma w(F_o^2-F_c^2)^2$	$\Sigma w(\lvert F_o\rvert-\lvert F_c\rvert)^2$
w	$1/[\sigma^2(F_o^2)+(0.1083P)^2+22.0586P]$ where $P=(F_o^2+2F_c^2)/3$	$1/\sigma^2(F_o)$
R ($I>2\sigma(I)$) [b]	0.059	0.051
wR_2 [c] (for **7**·C_3H_6O) and wR (for **10**)	0.155	0.045
GOF	1.04	1.19
Residuals in final difference map (e Å^{-3})	2.90, −2.86	0.70, −1.19

[a] Extended by 25% on both sides for background measurements.
[b] $R = \Sigma\lVert F_o\rvert-\lvert F_c\rVert/\Sigma\lvert F_o\rvert$.
[c] $wR_2 = \{\Sigma[w(F_o^2-F_c^2)^2]/\Sigma(wF_o^2)^2\}^{1/2}$ and $wR = \{\Sigma w(\lvert F_o\rvert-\lvert F_c\rvert)^2/\Sigma wF_o^2\}^{1/2}$.

2.6.2. *(t-BuNC)(PPh$_3$)Pt(μ-η^1:η^2-C=C(Ph)N-(S(O)$_2$Tol-p)C(O)CH$_2$)Ru(CO)Cp* (**10**)

Crystals of **10** were grown from dichloromethane–hexane. The data collection crystal, a yellow plate, was glued to the inside surface of a glass capillary. A small amount of a dichloromethane–hexane mixture was also sealed inside the capillary. The unit cell constants were determined by a least-squares fit of the diffractometer setting angles for 25 reflections in the 2θ range 29–30° with Mo–K_α radiation on a Rigaku AFC5S diffractometer.

Six standard reflections were measured after every 150 reflections during data collection and indicated that the crystal was undergoing decay. Four of the standards were low angle reflections ($2\theta < 10°$) and showed a percentage decrease in intensity in the range 5.3–8.2%. The other two standards were high angle ($2\theta \simeq 30°$) and exhibited much larger decreases in intensity, 28.1–30.7%. Data reduction was done with the TEXSAN package [20]. A decay correction was applied based on an average decrease in intensity of 14.3%. The data was also corrected for absorption by the empirical ψ scan method [21].

The Pt and Ru atoms were located by the Patterson method. The rest of the molecule was elucidated by use of the DIRDIF procedure [22] and standard Fourier methods. Full-matrix least-squares refinements on F were performed in TEXSAN [20]. The Cp ring appeared to be disordered and was modeled in terms of two orientations within a common plane: C(37), C(38), C(39), C(40) and C(41) label one ring, while C(37A), C(38A), C(39A), C(40A) and C(41A) label the other. Each ring has a fixed occupancy factor of 0.5. The t-Bu group also appeared to be disordered with respect to rotation about the N(2)–C(36) bond, and was modeled with two sets of Me carbons: C(44), C(45) and C(46) define one set, and C(47), C(48) and C(49) define the second set. Each set has an occupancy factor fixed at 0.5. Both the Cp ring and the Me carbons of the t-Bu group were refined isotropically, while all the other non-hydrogen atoms were refined anisotropically. Hydrogen atoms were included in the model as fixed contributions based on calculated positions at C–H = 0.98 Å and $B_H = 1.2B_{eq}$ (attached carbon atom).

Methyl group hydrogen atoms were idealized to sp^3 geometry based on positions located on various difference electron density maps. There are no hydrogens on the Me carbon C(46), as no reasonable positions for defining hydrogen atoms could be located on a ΔF map. The final refinement cycle was based on the 4763 intensities with $I > 2\sigma(I)$. Scattering factors for the non-hydrogen atoms, including terms for anomalous dispersion [23], and the scattering factor for the hydrogen atom [24] are from the literature. A summary of the crystal data and the details of the intensity data collection and refinement are provided in Table 1.

3. Results and discussion

3.1. Reactions of $(PPh_3)_2Pt(\mu\text{-}\eta^1\text{:}\eta^2_{\alpha,\beta}\text{-}C(R)\text{=}C\text{=}CH_2)Ru(CO)Cp$ (R = H (1), Ph (2)) with nucleophilic reagents

Reaction of **1** and **2** with $Ph_2PCH_2CH_2CH_2PPh_2$ in THF first at −78°C and then at r.t. afforded the substitution products $(Ph_2PCH_2CH_2CH_2PPh_2)Pt(\mu\text{-}\eta^1\text{:}\eta^2_{\alpha,\beta}\text{-}C(R)\text{=}C\text{=}CH_2)Ru(CO)Cp$ (R = H (**3**), Ph (**4**)) as yellow solids (Eq. (2)).

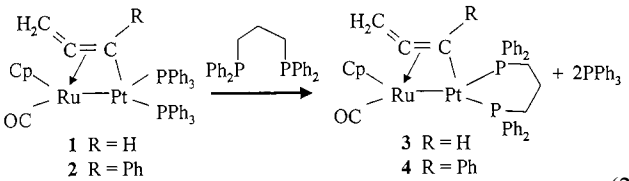

(2)

The substitution was shown to proceed cleanly by NMR spectroscopy; however, the yields of isolated products are only 40–50% owing to the difficulty in complete removal of triphenylphosphine.

Complexes **3** and **4** were characterized by a combination of IR and NMR (^1H, $^{13}C\{^1H\}$ and $^{31}P\{^1H\}$) spectroscopy, FAB mass spectrometry and chemical analysis. The IR ν(CO) absorption at 1902–1901 cm^{-1} is about 10 cm^{-1} lower than that of **1** or **2**, consistent with replacement of two PPh_3 ligands with a stronger base $Ph_2PCH_2CH_2CH_2PPh_2$. The ^1H- and $^{13}C\{^1H\}$-NMR spectra (cf. Section 2) show that the Ru(CO)Cp fragment remained intact. The $\mu\text{-}\eta^1\text{:}\eta^2_{\alpha,\beta}$-allenyl also retains its integrity in the reaction, as reflected by its characteristic ^1H- and $^{13}C\{^1H\}$-NMR signals. Thus, the $=CH_2$ protons are inequivalent and resonate at δ 5.59 and 4.77 for **3** and δ 6.12 and 5.56 ($^2J_{HH} = 2.2$ Hz) for **4**. The =CH proton of **3** occurs at δ 6.70. The $^{13}C\{^1H\}$ signals are observed at δ 168.9 (=C=), 112.4 (=CH, $J_{PtC} = 722$ Hz) and 94.5 ($=CH_2$). These data are very similar to those of the parent complexes **1** and **2** [17]. In the $^{31}P\{^1H\}$-NMR spectra of **3** and **4**, the two P nuclei are inequivalent, as they are for **1** and **2**, and couple differently to ^{195}Pt ($J_{PtP} = 2564$ and 3406 Hz for **3**, $J_{PtP} = 2526$ and 3427 Hz for **4**). Again these features are very reminiscent of those of the μ-allenyl precursors. The appearance in the FAB mass spectra of a peak corresponding to $Pt(Ph_2P(CH_2)_3PPh_2)^+$, as well as the presence in the ^1H- and $^{13}C\{^1H\}$-NMR spectra of the appropriate resonances of $CH_2CH_2CH_2$, indicate that phosphine substitution indeed occurred at platinum.

Complexes **3** and **4** are much less reactive than **1** and **2**. For example, neither **3** nor **4** reacts with CO in benzene at ca. 70°C in 2–4 days. Likewise, no reaction was observed between **3** and *t*-BuNC in THF at reflux temperature for 18 h. In contrast, under less forcing conditions, reactions do occur for **1** and/or **2** with CO and *t*-BuNC and lead to replacement of PPh_3 by the reacting ligand or to fragmentation of the binuclear complex [17].

Treatment of **1** with PEt_3 (either two equivalents or an excess) in THF under conditions comparable with those for the reactions of **1** and **2** with $Ph_2PCH_2CH_2CH_2PPh_2$ leads to the formation of $(PEt_3)_2Pt(\mu\text{-}\eta^1\text{:}\eta^2_{\alpha,\beta}\text{-}CH\text{=}C\text{=}CH_2)Ru(CO)Cp$ (**5**) (Eq. (3)), isolated in 85% yield as a yellow solid.

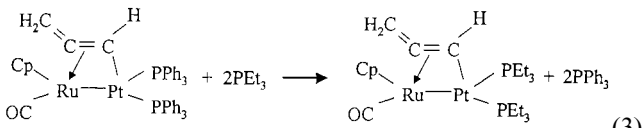

(3)

The product exhibits spectroscopic properties that are very similar to those of **1**–**4**. Accordingly, the IR ν(CO) absorption at 1892 cm^{-1} reflects stronger basicity of PEt_3 than of PPh_3 or $Ph_2PCH_2CH_2CH_2PPh_2$. In the ^1H-NMR spectrum of **5** the =CH resonance is observed at δ 6.42 as a multiplet, while the inequivalent $=CH_2$ protons are seen at δ 5.41 and 4.70, also as multiplets owing to spin–spin coupling with phosphorus. All three protons are coupled to ^{195}Pt ($J_{PtH} = 31$, 20 and 13 Hz, respectively). The two PEt_3 ligands are, as expected [17], inequivalent in the $^{31}P\{^1H\}$-NMR spectrum, giving rise to signals at δ 23.9 and 12.4 with $J_{PP} < 1$ Hz and $J_{PtP} = 3681$ and 2733 Hz, respectively. A parent mass peak, m/z 665, is observed in the FAB spectrum.

The reaction of **2** with an excess of *t*-BuNC in THF, first at −78°C and then at r.t., afforded the monosubstitution product $(t\text{-BuNC})(PPh_3)Pt(\mu\text{-}\eta^1\text{:}\eta^2_{\alpha,\beta}\text{-}C(Ph)\text{=}C\text{=}CH_2)Ru(CO)Cp$ (**6**) (Eq. (4)) as a yellow solid in 67% yield.

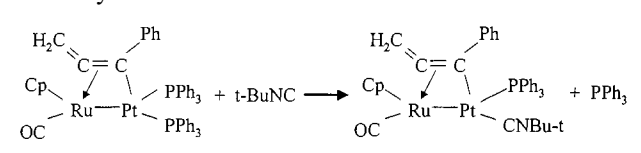

(4)

The second PPh_3 ligand could not be replaced even upon heating for several hours at ca. 67°C. Complex **6** is rather unusual in that all of its ligands and the two metals are different. It was unambiguously characterized by IR and NMR (^1H, $^{13}C\{^1H\}$ and $^{31}P\{^1H\}$) spectroscopy, FAB mass spectrometry and elemental analysis. The IR ν(CO) absorption at 1901 cm^{-1} shows higher electron density at ruthenium in **6** than in **2**, as a result of replacement of PPh_3 with the more basic *t*-BuNC at platinum. The $=CH_2$ protons observed at δ 5.62 and 4.98 are not discernibly coupled to each other or to phosphorus, but are coupled to ^{195}Pt ($J_{PtH} = 17$ and 13 Hz, respectively). The $^{13}C\{^1H\}$-NMR spectrum displays rather typical resonances for the three μ-allenyl carbons at δ 166.5 (=C=), 150.1 (=*C*Ph) and 97.0 ($=CH_2$, $J_{PtH} = 32.2$ Hz). The lone $^{31}P\{^1H\}$-NMR signal is observed at δ 25.6 with $J_{PtP} = 3544$ Hz; the magnitude of the latter suggests that the Ph_3P–Pt bond is positioned *trans* to Ru–Pt [10,17]. Additional evidence for this stereochemical feature comes from the structural analysis of complex **10**, which will be presented in Section 3.2.1. The FAB mass spectrum of **6** shows a strong molecular ion peak at m/z 850.

Unlike $Ph_2PCH_2CH_2CH_2PPh_2$, PEt_3 and *t*-BuNC, which reacted with substitution at the Pt center of **1** and **2**, the nitrogen-donor ligands Et_2NH, $C_6H_{11}NH_2$ and *p*-$TolS(O)_2NH_2$ failed to react with **1** or **2** in THF or benzene solution even at elevated temperatures. This selectivity reflects a greater preference of platinum for the softer ligands phosphine and isocyanide than for the harder amines.

The results obtained here may be contrasted with those of Carty [4,5] and Doherty [6–9], who have reported a number of reactions of $(CO)_3Ru(\mu\text{-}PPh_2)$-$(\mu\text{-}\eta^1{:}\eta^2_{\alpha,\beta}\text{-}C(Ph){=}C{=}CH_2)Ru(CO)_3$, $(CO)_3Ru(\mu\text{-}PPh_2)$-$(\mu\text{-}\eta^1{:}\eta^2_{\alpha,\beta}\text{-}C(Ph){=}C{=}CPh_2)Ru(CO)_3$, $(CO)_3Fe(\mu\text{-}PPh_2)$-$(\mu\text{-}\eta^1{:}\eta^2_{\alpha,\beta}\text{-}C(R){=}C{=}CH_2)Fe(CO)_3$ (R = H, Ph) and $(CO)_3Fe(\mu\text{-SBu-}t)(\mu\text{-}\eta^1{:}\eta^2_{\alpha,\beta}\text{-}CH{=}C{=}CH_2)Fe(CO)_3$ with nucleophilic reagents. They found that the aforementioned μ-allenyl complexes are quite electrophilic and readily react with primary amines [4a,7], alcohols [8], organolithium reagents [9a], isocyanides [4a,9b], phosphite esters [4a,6b] and monodentate and bidentate phosphines [4–6]. In most cases, the nucleophile adds to the allenyl ligand; however, addition to carbon monoxide and metal also has been noted. By way of contrast, complexes **1** and **2** do not display such electrophilic properties, and their reactions with nucleophilic reagents appear to be limited to substitution at the relatively labile platinum center. The much more pronounced electrophilic properties of the Carty–Doherty μ-allenyls may be attributed to the presence of six good π-acid CO ligands in those complexes. The presence of only one CO in conjunction with the considerably weaker π-acceptor Cp and PPh_3 ligands renders complexes **1** and **2** appreciably more nucleophilic. The results discussed in the next section reinforce this generalization further.

3.2. Reactions of $L_2Pt(\mu\text{-}\eta^1{:}\eta^2_{\alpha,\beta}\text{-}C(R){=}C{=}CH_2)$-$Ru(CO)Cp$ ($L_2 = 2PPh_3$, R = H (**1**), Ph (**2**); $L_2 = Ph_2PCH_2CH_2CH_2PPh_2$, R = H (**3**), Ph (**4**); $L_2 = PPh_3$ and *t*-BuNC, R = Ph (**6**)) with electrophilic reagents

As was stated in Section 1, complexes **1** and **2** react with the electrophilic species $(PPh_3)Au^+$ to afford trimetallic η^3-allyl cations by addition of gold phosphine to the β-carbon atom of the μ-allenyl ligand [10]. To explore the generality and scope of the electrophilic reactions of **1**, **2** and related complexes, we have extended our investigation to various unsaturated electrophiles, especially isocyanates, alkenes and alkynes. We begin our presentation with reactions between complexes **1**–**4**, **6** and *p*-$TolS(O)_2NCO$. *p*-Toluenesulfonyl isocyanate was previously shown to react with mononuclear transition-metal η^1-allyls, propargyls and allenyls (Eq. (5)) to afford [3 + 2] cycloaddition products [16,25,26].

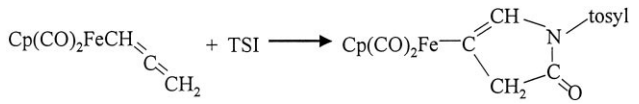

(5)

Furthermore, cycloaddition reactions with the η^1-allyl and propargyl complexes were found to proceed sufficiently cleanly to be amenable to kinetic studies [16,26].

3.2.1. Reactions of **2**, **4** and **6** with *p*-$TolS(O)_2NCO$ (TSI)

Reaction of **2** with an excess of TSI in toluene first at − 78°C and then at r.t. afforded two bimetallic products: yellow $(PPh_3)_2Pt(\mu\text{-}\eta^1{:}\eta^2_{\alpha,\beta}\text{-}C(Ph){=}C{=}CHC(O)NHS(O)_2Tol\text{-}p)Ru(CO)Cp$ (**7**), isolated in 54% yield, and orange $(PPh_3)_2Pt(\mu\text{-}\eta^1{:}\eta^2\text{-}C{=}C(Ph)N(S(O)_2Tol\text{-}p)C(O)CH_2)Ru(CO)Cp$ (**8**), obtained in ca. 11% yield (Eq. (6)).

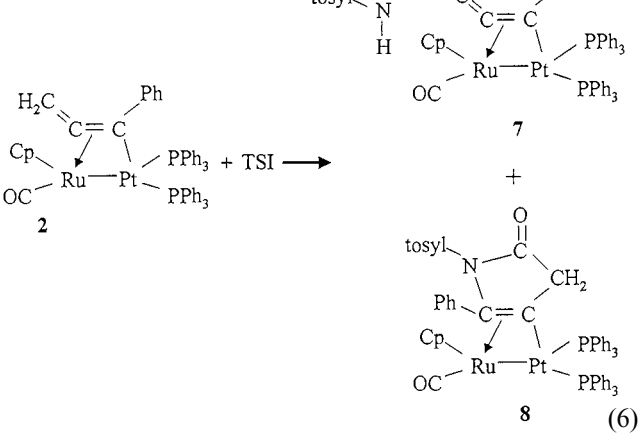

(6)

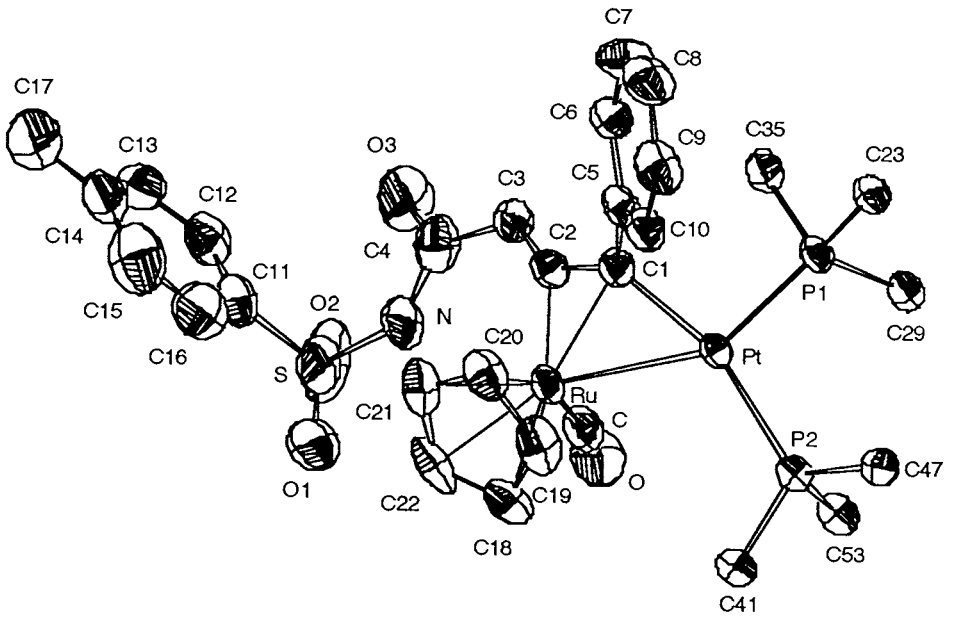

Fig. 1. ORTEP plot of **7** in $7{\cdot}C_3H_6O$. The non-hydrogen atoms are drawn at the 50% probability level. For clarity only the P-bonded carbon atoms of the PPh_3 groups are shown, and the hydrogen atoms are omitted.

Complex **7** precipitated from the reaction solution, whereas **8** was isolated from the mother liquor.

That the Pt–Ru bond remains intact in **7** is evident upon examination of the ν(CO) region of the IR spectrum (1924 (s), 1670 (s) cm^{-1}) and the signals in the $^{31}P\{^1H\}$-NMR spectrum (21.6, $J_{PP} = 11$ Hz, $J_{PtP} = 2789$ Hz and 20.9, $J_{PP} = 11$ Hz, $J_{PtP} = 3923$ Hz). The former shows CO groups bonded to ruthenium and nitrogen, respectively, and the latter indicate that the phosphorus atoms of PPh_3 on platinum are inequivalent and resonate with the appropriate coupling constants. The ^1H-NMR spectrum reveals NH (δ 12.1) and CH (δ 5.96, $J_{PtH} = 10$ Hz) protons and the Me group of the *p*-TolS(O)$_2$ substituent (δ 2.43), all as singlets, to suggest an interaction between μ-allenyl and a TSI-derived fragment. The $^{13}C\{^1H\}$-NMR signals at δ 164.5, 146.2 and 108.4 are very similar to those for the parent complex **2** (δ 165.3, 149.1 and 97.2). Further evidence for the formulation of **7** comes from the FAB mass spectrum, which shows a molecular ion peak at m/z 1226, and from elemental analysis.

However, to unequivocally establish the structure of **7** an X-ray diffraction analysis was carried out. The crystal consists of PtRu binuclear molecules (**7**) and acetone of crystallization in a 1:1 ratio. The molecular structure of **7** appears in Fig. 1, and selected bond distances and angles are provided in Table 2.

Molecules of **7** are comprised of Ru(CO)Cp and $Pt(PPh_3)_2$ fragments joined by a Pt–Ru single bond that is supported by a bridging μ-η^1:$\eta^2_{\alpha,\beta}$-C(Ph)=C=CHC(O)NHS(O)$_2$Tol-*p* ligand. This new μ-allenyl ligand resulted from the addition of *p*-TolS(O)$_2$NCO through the NCO carbon to γ-carbon of the parent μ-η^1:$\eta^2_{\alpha,\beta}$-C(Ph)=C=CH_2. The addition was accompanied by a proton transfer from the =CH_2 carbon of **2** to the isocyanate nitrogen. The connectivity of μ-allenyl to

Table 2
Selected bond distances (Å), bond angles (°) and torsion angles (°) for $(PPh_3)_2Pt(\mu\text{-}\eta^1\text{:}\eta^2_{\alpha,\beta}\text{-C(Ph)=C=CHC(O)NHS(O)}_2\text{Tol-}p)\text{Ru(CO)Cp}\cdot C_3H_6O$ (**7**·C_3H_6O)

Bond distances			
Pt–Ru	2.7009(8)	CO	1.137(13)
Pt–P(1)	2.260(2)	C(4)–O(3)	1.210(14)
Pt–P(2)	2.296(2)	C(4)–N	1.37(2)
Pt–C(1)	2.028(9)	C(1)–C(2)	1.378(12)
Ru–C	1.854(11)	C(1)–C(5)	1.490(12)
Ru–C(1)	2.147(9)	C(2)–C(3)	1.354(13)
Ru–C(2)	2.053(9)	C(3)–C(4)	1.45(2)
Bond angles			
C(1)–Pt–P(1)	98.0(3)	C(2)–C(1)–C(5)	123.3(8)
C(1)–Pt–P(2)	159.2(3)	C(2)–C(1)–Pt	117.6(6)
P(1)–Pt–P(2)	102.15(8)	C(5)–C(1)–Pt	119.1(6)
C(1)–Pt–Ru	51.6(2)	C(2)–C(1)–Ru	67.2(5)
P(1)–Pt–Ru	147.86(6)	C(5)–C(1)–Ru	123.9(6)
P(2)–Pt–Ru	109.24(6)	C(1)–C(2)–C(3)	140.6(9)
C–Ru–C(1)	98.6(4)	C(3)–C(2)–Ru	144.6(7)
C–Ru–C(2)	85.5(4)	C(1)–C(2)–Ru	74.6(6)
C–Ru–Pt	70.6(3)	C(2)–C(3)–C(4)	126(1)
C(1)–Ru–Pt	47.8(2)	O(3)–C(4)–N	121(1)
C(2)–Ru–Pt	74.8(3)	O(3)–C(4)–C(3)	123(1)
O–C–Ru	174(1)	N–C(4)–C(3)	115.4(9)
Torsion angles			
C(5)–C(1)–C(2)–C(3)	67(2)		
Pt–C(1)–C(2)–C(3)	−111(1)		
Ru–C(1)–C(2)–C(3)	−176(2)		
C(5)–C(1)–C(2)–Ru	−116.6(9)		
C(1)–C(2)–C(3)–C(4)	−179(1)		
Ru–C(2)–C(3)–C(4)	8(2)		

Pt–Ru remained unchanged and is through C(1) to Pt and through the internal C=C (C(1) and C(2)) to Ru. The remaining structural features of **7** are remarkably similar to those found in **1** and/or $(PPh_3)(CO)Pt(\mu\text{-}\eta^1{:}\eta^2_{\alpha,\beta}\text{-}C(Ph){=}C{=}CH_2)Ru(CO)Cp$ (**I**), and its relevant metrical parameters are also comparable [17].

The Pt–Ru bond distance of 2.7009(8) Å is somewhat shorter than that of 2.718(1) Å in **1**, but longer than that of 2.668(1) Å in **I**. The Ru–C(allenyl) bond lengths in **7** are Ru–C(1) = 2.147(9) Å and Ru–C(2) = 2.053(9) Å; for comparison, $Ru–C_\alpha = 2.116(6)$ Å and $RuC_\beta = 2.098(7)$ Å in **1**, and $Ru–C_\alpha = 2.162(9)$ Å and $RuC_\beta = 2.107(8)$ Å in **I**. The Pt–C(1) bond distance 2.028(9) Å in **7** may be compared with that of 2.015(6) Å in **1** and 2.025(9) Å in **I**. The $\mu\text{-}\eta^1{:}\eta^2_{\alpha,\beta}$-allenyl ligand displays carbon–carbon bond distances (C(1)–C(2) = 1.378(12) and C(2)–C(3) = 1.354(13) Å) that are in the normal range for this type of bonding with $C_\alpha–C_\beta > C_\beta–C_\gamma$ [2]. The allenyl C(1)–C(2)–C(3) bond angle of 140.6(9)° is somewhat less obtuse than that observed in similarly bonded compounds [2,9a].

The atoms P(1), P(2), Ru and C(1) provide a distorted planar coordination environment around the Pt center, with the bond angles being P(1)–Pt–P(2) 102.15(8)°, C(1)–Pt–Ru 51.6(2)°, C(1)–Pt–P(1) 98.0(3)° and P(2)–Pt–Ru 109.24(6)°. The two Pt–P bond distances are slightly different: Pt–P(1) = 2.260(2) and Pt–P(2) = 2.296(2) Å. A somewhat longer Pt–P bond *trans* to the bridging hydrocarbyl α-carbon (C(1)) than that *trans* to ruthenium appears to be a general phenomenon in these heterobinuclear and heterotrinuclear $RuPt(PPh_3)_2$-fragment containing μ-allenyl and related complexes [10,17]. Significantly, it is the phosphine approximately *trans* to that carbon atom (C(1)–Pt–P(2) 159.2(3)°) that undergoes facile substitution by other ligands, e.g. CO [17] and *t*-BuNC.

Complex **8**, the other product of the reaction in Eq. (6), is assigned a cycloaddition structure on the basis of spectroscopic similarities to the structurally characterized **10** (vide infra). The IR ν(CO) bands at 1899 (s) and 1724 (s) cm^{-1} are consistent with the presence of a ruthenium-bonded CO and a butenolactone ring [25b], respectively. The position and the splitting of the ^1H- and $^{13}C\{^1H\}$-NMR signals of the methylene group indicate that this CH_2 is considerably different from the $=CH_2$ of the precursor **2**. Thus, the $^{13}C\{^1H\}$ resonance occurs as a singlet at δ 52.5 ($J_{PtC} = 54.7$ Hz), shifted upfield from δ 97.2 in **2**, in line with the hybridization changing from sp^2 to sp^3. An AB/ABX splitting pattern in the ^1H-NMR spectrum (δ 3.71, $^2J_{HH} = 21.3$ Hz, $J_{PtH} = 17.2$ Hz and 2.72 Hz, $^2J_{HH} = 21.3$ Hz, $J_{PH} = 14.5$ Hz) implicates C_{sp^3}-bonded geminal protons that are rendered inequivalent by the absence of a symmetry plane in the molecule. The two PPh_3 phosphorus nuclei are predictably inequivalent (δ 22.7 and 16.3) and show J_{PtP} values (2643 and 3621 Hz, respectively) typical for these PtRu complexes [10,17].

Complex **4** reacted with excess TSI in benzene at r.t. to produce $(Ph_2PCH_2CH_2CH_2PPh_2)Pt(\mu\text{-}\eta^1{:}\eta^2\text{-}C{=}C\text{-}(Ph)N(S(O)_2Tol\text{-}p)C(O)CH_2)Ru(CO)Cp$ (**9**) (Eq. (7)) as a yellow solid in 53% yield.

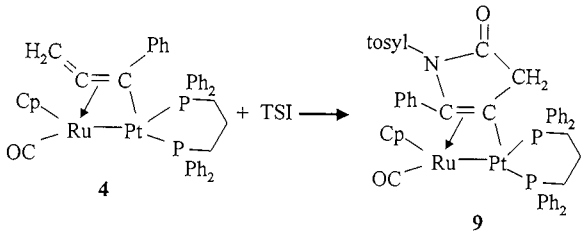

(7)

No product structurally analogous to **7** was observed in this reaction. Salient spectroscopic features of **9** include IR ν(CO) absorptions at 1894 (s) and 1708 (m) cm^{-1}, inequivalent NMR signals of the CH_2 protons at δ 3.41 and 2.82 and two $^{31}P\{^1H\}$ resonances at δ 0.47 ($J_{PtP} = 2362$ Hz) and −6.6 ($J_{PtP} = 3468$ Hz) showing mutual coupling ($J_{PP} = 26.5$ Hz) of the phosphorus nuclei. The FAB mass spectrum shows a peak at m/z 1114, consistent with the complex being a 1:1 adduct of **4** and TSI. These data support a structure similar to that of **8**.

Treatment of **6** with a two-fold excess of TSI in toluene at −78°C, followed by warming and continued reaction at r.t., resulted in the isolation of yellow $(t\text{-}BuNC)(PPh_3)Pt(\mu\text{-}\eta^1{:}\eta^2\text{-}C{=}C(Ph)N(S(O)_2Tol\text{-}p)\text{-}C(O)CH_2)Ru(CO)Cp$ (**10**) in 60% yield (Eq. (8)).

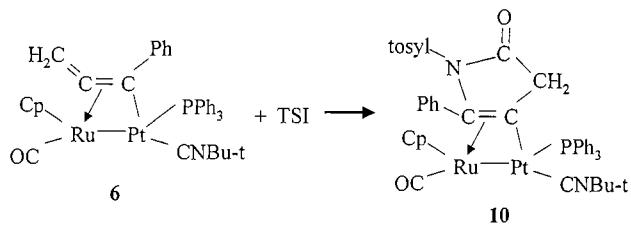

(8)

Spectroscopic data for **10**, furnished in Section 2, show many similarities to those for **8** and **9**. The CH_2 protons are inequivalent (δ 3.66, $J_{PH} = 1.8$ Hz, $J_{PtH} = 50$ Hz and 3.29, $J_{PH} = 6.6$ Hz) and mutually coupled ($^2J_{HH} = 21.6$ Hz). The μ-allenyl-derived carbon atoms resonate at δ 167.7 (=CPt), 141.1 (=*C*Ph) and 52.7 (CH_2), close to the chemical shift values reported for [3 + 2] cycloaddition-derived butenolactone complexes and for products of related cycloaddition reactions [16,27,28]. The FAB mass spectrum features a parent molecular ion peak at m/z 1047 and, most interestingly, a peak at m/z 850. The latter corresponds to $(M^+–TolS(O)_2NCO)$ and occurs with relative intensity = 100 to indicate that the cycloaddition reaction of **6** with TSI is readily reversed for $\mathbf{10}^+$ in the gas phase.

Unequivocal determination of the structure of **10** was achieved by an X-ray diffraction analysis. The molecular structure is shown in Fig. 2, and selected bond

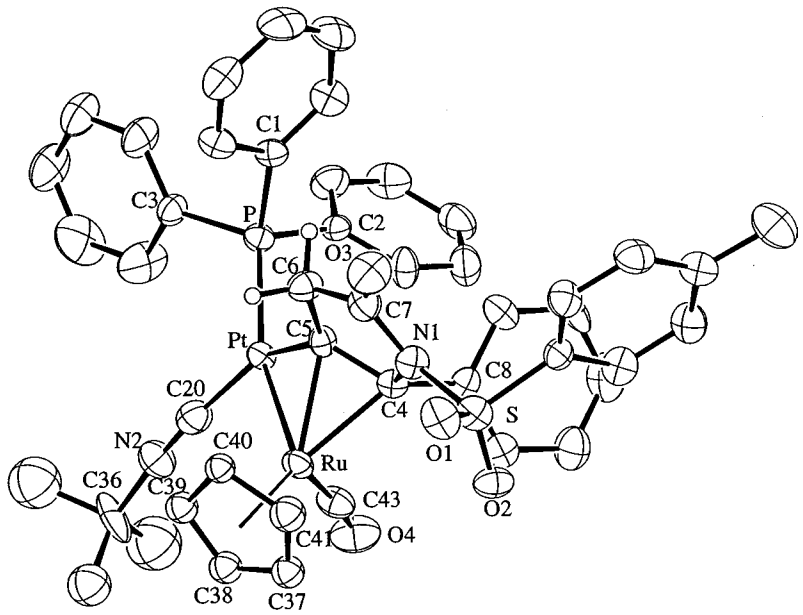

Fig. 2. ORTEP plot of **10**. The non-hydrogen atoms are represented by 30% probability thermal ellipsoids. The hydrogen atoms have been omitted for clarity, except the two hydrogens bonded to C(6). Only one orientation of the disordered Cp ring and one set of methyl carbons on the disordered *t*-butyl group are shown.

distances and angles are given in Table 3. The most striking feature of **10** is the presence of a bridging butenolactone group, which was formed by [3 + 2] cycloaddition of TSI to the μ-allenyl ligand of **6**. The butenolactone is η^2 bonded to Ru (Ru–C(4) = 2.150(9) and Ru–C(5) = 2.153(10) Å) and η^1 bonded to Pt (Pt–C(5) = 1.983(9) Å). These bond distances are unexceptional.

The generated C_4N five-membered ring is essentially planar (deviation from the least-squares plane: N(1) 0.0228, C(4) −0.0368, C(5) 0.0345, C(6) −0.0218, C(7) 0.0128, mean 0.0257 Å), and its bond distances are normal. Thus, C(5)–C(6) = 1.526(14) and C(6)–C(7) = 1.518(14) Å correspond to carbon–carbon single bonds, while C(4)–C(5) = 1.447(12) Å is in line with a metal-coordinated carbon–carbon double bond [29]. The carbon–nitrogen bond distances C(4)–N(1) = 1.497(12) and C(7)–N(1) = 1.390(14) Å are respectively representative of a single bond [30] and a single bond shortened by contribution from the resonance representation N(1)=C(7)–O(3).

The coordination environment around the platinum center is distorted planar, with C(5) being displaced −0.154 Å from the 'best' four-atom plane PtRuPC(20) (mean deviation 0.015 Å). This plane makes an angle of 61.6(5)° with the butenolactone ring. The four-coordinate environment of platinum is characterized by the following bond angles: P–Pt–C(20) 100.3(3), Ru–Pt–C(5) 52.8(3), Ru–Pt–C(20) 100.3(3) and P–Pt–C(5) 106.7(3)°. The corresponding bond distances are Pt–Ru = 2.664(1), Pt–P 2.271(3), Pt–C(20) = 1.964(13) and Pt–C(5) = 1.983(9) Å. The Pt–Ru bond distance may be compared with those in the range 2.668(1)–2.718(1) Å for the μ-allenyl complexes **1**, **7**

Table 3
Selected bond distances (Å) and angles (°) for (*t*-BuNC)(PPh_3)Pt(μ-η^1:η^2-C=C(Ph)N($S(O)_2$Tol-*p*)C(O)CH_2)Ru(CO)Cp (**10**)

Bond distances			
Pt–Ru	2.664(1)	N(1)–C(4)	1.497(12)
Pt–P	2.271(3)	N(1)–C(7)	1.390(14)
Pt–C(5)	1.983(9)	N(2)–C(20)	1.151(13)
Pt–C(20)	1.964(13)	N(2)–C(36)	1.480(15)
Ru–C(4)	2.150(9)	C(4)–C(5)	1.447(12)
Ru–C(5)	2.153(10)	C(4)–C(8)	1.515(13)
Ru–C(43)	1.836(12)	C(5)–C(6)	1.526(14)
O(4)–C(43)	1.152(12)	C(6)–C(7)	1.518(14)
Bond angles			
Ru–Pt–P	159.34(7)	Ru–C(4)–C(5)	70.5(6)
Ru–Pt–C(5)	52.8(3)	N(1)–C(4)–C(5)	106.5(8)
Ru–Pt–C(20)	100.3(3)	Pt–C(5)–Ru	80.1(4)
P–Pt–C(5)	106.7(3)	Pt–C(5)–C(4)	125.0(7)
P–Pt–C(20)	100.3(3)	Pt–C(5)–C(6)	127.6(7)
C(5)–Pt–C(20)	152.8(4)	Ru–C(5)–C(4)	70.2(6)
Pt–Ru–C(4)	77.9(2)	Ru–C(5)–C(6)	120.5(7)
Pt–Ru–C(5)	47.1(2)	C(4)–C(5)–C(6)	107.3(8)
Pt–Ru–C(43)	75.3(4)	C(5)–C(6)–C(7)	106.9(9)
C(4)–Ru–C(5)	39.3(3)	O(3)–C(7)–N(1)	126.4(11)
C(4)–Ru–C(43)	91.9(4)	O(3)–C(7)–C(6)	127.1(11)
C(5)–Ru–C(43)	102.6(4)	N(1)–C(7)–C(6)	106.4(10)
C(4)–N(1)–C(7)	112.5(9)	Pt–C(20)–N(2)	173.8(11)
C(20)–N(2)–C(36)	175.3(13)	Ru–C(43)–O(4)	172.2(11)
Ru–C(4)–N(1)	114.4(6)		

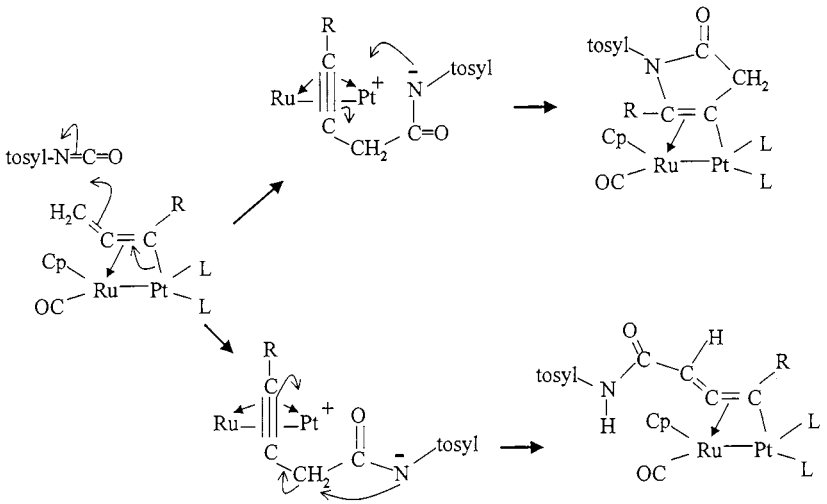

Scheme 1.

and **I** [17]. The Pt–P [31], Pt–C_{sp^2} [17] and Pt–C_{sp} [32] bond lengths are normal. Interestingly, the PPh_3 ligand is positioned approximately *trans* to Ru (Ru–Pt–P 159.34(7)°), and *t*-BuNC is approximately *trans* to C(5) (C(5)–Pt–C(20) 152.8(4)°). If the same stereochemistry characterizes the precursor complex **6** — and there is spectroscopic evidence for it (cf. Section 3.1) — then substitution of *t*-BuNC for PPh_3 in **2** (Eq. (4)) proceeds stereoselectively at the platinum site *trans* to the hydrocarbyl carbon. Studies of ligand substitution reactions of **1** and **2** suggest that this may be a general phenomenon [17].

Reactions of complexes **1** and **3** with TSI under a variety of conditions were investigated by ^{1}H- and ^{31}P{^{1}H}-NMR spectroscopy and found to yield products strictly analogous to those obtained from the Ph-substituted PtRu analogs **2** and **4**. However, in addition to the products differing from **7**–**9** only by replacement of Ph with H, a number of other, uncharacterized binuclear and mononuclear metal-containing species were detected in solution. The complexes could not be successfully separated by chromatography, and studies on these systems were not further pursued.

The formation of complexes **7**–**10** may be rationalized by a mechanism similar to that proposed for reactions of metal η^1-allyl, propargyl and allenyl complexes with unsaturated electrophilic reagents [33]. A suitable adaptation of the latter for the binuclear PtRu μ-η^1:$\eta^2_{\alpha,\beta}$-allenyl complexes and TSI is depicted in Scheme 1. Electrophilic attack of TSI, through the carbonyl carbon, at the uncoordinated C=CH_2 bond of μ-allenyl leads to the formation of a zwitterionic PtRu alkyne intermediate, in which the alkyne bonds in a perpendicular mode to both Ru and Pt (all ancillary ligands are omitted for clarity in Scheme 1). This intermediate is similar to that (**II**) proposed for [3 + 2] cycloaddition of TSI to $Cp(CO)_2FeCH{=}C{=}CH_2$ (Eq. (5)) [25b].

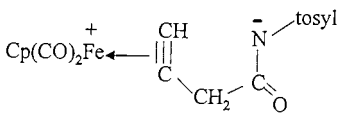

II

Collapse of the PtRu μ-alkyne intermediate by attack of the negative nitrogen terminus at the $\equiv CR$ carbon, with rearrangement of Pt-η^2-$C(R){\equiv}CCH_2$ to Pt-η^1-$C(=CR)CH_2$, affords the [3 + 2] cycloaddition product. Alternatively, the intermediate undergoes proton transfer to the nitrogen to generate the *p*-$TolS(O)_2NHC(O)$-substituted μ-η^1:$\eta^2_{\alpha,\beta}$-allenyl complex. The latter pathway occurs, together with the cycloaddition route, in the reaction of **2** with TSI. It is precedented by the behavior of $Cl_3CC(O)NCO$ toward the η^1-allyl complex $Cp(CO)_2FeCH_2CH{=}CH_2$ resulting in the formation of $Cp(CO)_2FeCH_2CH{=}CHC(O)NHC(O)CCl_3$ [25c].

The mechanism in Scheme 1 shows an interesting example of metal cooperativity in effecting the formation of products. Platinum appears to be the more involved metal atom in the reaction by undergoing a bonding change from the Pt-η^1-C mode in the μ-allenyl complex to a Pt^+-η^2-(C≡C) attachment in the zwitterionic intermediate. The positive charge that develops on the platinum as a result of this conversion renders the C≡C more vulnerable to addition, and the CH_2 protons more susceptible to abstraction by the negative nitrogen. The role of the ruthenium atom in these transformations may be to help stabilize the Pt^+-η^2-(C≡C) interaction in the intermediate, and thus promote attack by nitrogen.

3.2.2. Reactions of **1** and **2** with other unsaturated organic compounds

Since TSI reacted with each of **2**, **4** and **6** to furnish stable addition products, it was of interest to ascertain whether other unsaturated electrophilic reagents would behave similarly. In that vein, reactions were examined between the electrophiles $ClS(O)_2NCO$ and TCNE and complexes **1** and **2**. Both of these electrophilic reagents are known to react with transition-metal η^1-allenyls to afford [3 + 2] cycloaddition complexes that are structurally analogous to the product in Eq. (5) [33]. However, the reaction of **2** with $ClS(O)_2NCO$ afforded only uncharacterized decomposition materials. The reaction of **1** with TCNE in CH_2Cl_2 at ca. − 78°C gave several products as shown by a $^{31}P\{^1H\}$-NMR spectrum; of these, two could be characterized as a binuclear $(PPh_3)_2PtRu$-containing species and known [15] $(PPh_3)_2Pt$(TCNE). Only the latter remained intact after the solution was allowed to warm to r.t.

The less electrophilic alkene $(CN)_2C{=}CPh_2$ was found to be unreactive toward **2** in benzene solution, even at reflux temperature. In contrast, the reaction of **2** with a two-fold excess of fumaronitrile in benzene, also at reflux, resulted in ca. 75% consumption of **2** after 24 h and the formation of $Cp(CO)_2RuC(Ph){=}C{=}CH_2$ (cf. Section 3.2.3 for characterization), known [15] $(PPh_3)_2Pt$(*trans*-NCCH=CHCN) and other unidentified materials (Eq. (9)): L = *trans*-NCCH=CHCN). The products were characterized without separation by ^1H- and $^{31}P\{^1H\}$-NMR spectroscopy.

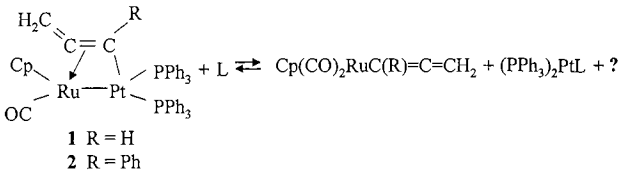

(9)

The second CO ligand of $Cp(CO)_2RuC(Ph){=}C{=}CH_2$ must originate from another molecule of **2**, and this transfer of CO is likely to be responsible for the decomposition observed in the reaction. Redistribution of CO also accounts for the approximate 2:1 ratio of $(PPh_3)_2Pt$(*trans*-NCCH=CHCN) to $Cp(CO)_2RuC(Ph){=}C{=}CH_2$ estimated by ^1H-NMR signal intensities.

Reactions of activated alkynes with **1** are similar to those of fumaronitrile with **2** (cf. Eq. (9)), except that they proceed at r.t. Thus, a 1:1 mixture of **1** and $MeO_2CC{\equiv}CCO_2Me$ in THF afforded after 12 h $Cp(CO)_2RuCH{=}C{=}CH_2$ and $(PPh_3)_2Pt(MeO_2CC{\equiv}CCO_2Me)$ [15], characterized by ^1H- and $^{31}P\{^1H\}$-NMR spectroscopy, in addition to other unidentified products. The reaction between 1:1 **1** and $MeO_2CC{\equiv}CMe$ in THF proceeded similarly at r.t. to give $Cp(CO)_2RuCH{=}C{=}CH_2$ and $(PPh_3)_2Pt(MeO_2CC{\equiv}CMe)$ [15], among other uncharacterized products. Only about 50% of **1** was consumed in 12 h.

A similar behavior was observed when the phenyl-substituted alkynes PhC≡CH and PhC≡CPh were allowed to react with **1** in THF solution under comparable conditions. Again, approximately 50% of **1** was consumed, and the products identified by ^1H- and $^{31}P\{^1H\}$-NMR spectroscopy were $Cp(CO)_2RuCH{=}C{=}CH_2$, $(PPh_3)_2Pt$(PhC≡CH) [15] or $(PPh_3)_2Pt$(PhC≡CPh) [15] and $Pt(PPh_3)_4$ [34]. There were, however, other, unassigned peaks in the NMR spectra.

That the reaction in Eq. (9) can also proceed in the reverse direction was demonstrated for L = PhC≡CPh. When $Cp(CO)_2RuCH{=}C{=}CH_2$ in $CDCl_3$ was treated with a slight deficiency of $(PPh_3)_2Pt$(PhC≡CPh) at r.t., and the resulting solution was stirred for several hours, unreacted $Cp(CO)_2RuCH{=}C{=}CH_2$ (the excess), **1** (> 95%) and a small amount of $(PPh_3)_2Pt$(PhC≡CPh) (< 5%) were detected in solution by ^1H- and $^{31}P\{^1H\}$-NMR spectroscopy. However, the reaction is not truly reversible, since the forward process is accompanied by some decomposition of the monocarbonyl **1** in producing the dicarbonyl $Cp(CO)_2RuCH{=}C{=}CH_2$.

The fragmentation of **1** upon treatment with PhC≡CPh may be contrasted with the reaction between $(CO)_3Ru(\mu\text{-}PPh_2)(\mu\text{-}\eta^1{:}\eta^2_{\alpha,\beta}\text{-}C(Ph){=}C{=}CH_2)Ru(CO)_3$ and PhC≡CPh, studied by Carty and co-workers [36]. The latter, conducted in toluene at reflux, resulted in a coupling of the allenyl and alkyne fragments with retention of both Ru atoms in the product complex.

3.2.3. Characterization of $Cp(CO)_2RuC(Ph){=}C{=}CH_2$

The allenyl product of the reaction in Eq. (9) (L = *trans*-NCCH=CHCN), $Cp(CO)_2RuC(Ph){=}C{=}CH_2$, represents a new organometallic compound. It can also be prepared by a similar reaction of **2** with CO in toluene as detailed in Section 2. Its isomer $Cp(CO)_2RuCH_2\text{-}C{\equiv}CPh$ was previously obtained from $Cp(CO)_2Ru^-$ and $PhC{\equiv}CCH_2Cl$ or $PhC{\equiv}CCH_2OS(O)_2Tol\text{-}p$ [16], and this propargyl complex has not been observed to undergo conversion to $Cp(CO)_2RuC(Ph){=}C{=}CH_2$.

Attempts at isolation and purification of $Cp(CO)_2RuC(Ph){=}C{=}CH_2$ from its reaction mixtures proved to be unsuccessful. However, NMR data obtained on such mixtures provided sufficient information for reliable characterization. Thus, the ^1H-NMR spectrum of $Cp(CO)_2RuC(Ph){=}C{=}CH_2$ shows the Cp and CH_2 resonances at δ 5.28 and 4.14, respectively. The position of these signals may be compared with those of the corresponding signals at δ 5.33 and 2.17 for $Cp(CO)_2RuCH_2C{\equiv}CPh$ [16], both recorded using $CDCl_3$ solution. The chemical shift of the CH_2 resonance at δ 4.14 is consistent with the presence of an $MC(R){=}C{=}CH_2$ fragment [16,35]. In the $^{13}C\{^1H\}$-NMR spectrum of $Cp(CO)_2RuC(Ph){=}C{=}CH_2$, resonances are observed at δ 206.6 for =C=, 68.1 for =*C*Ph and 61.8 for $=CH_2$. These data are in excellent agreement with those for $Cp(CO)_2RuCH{=}C{=}CH_2$, with the signal at δ 206.6 being particularly diagnostic for mononuclear metal η^1-allenyl complexes [16].

Efforts were also made to characterize $Cp(CO)_2RuC(Ph)=C=CH_2$ by conversion to a [3 + 2] cycloaddition product with TSI. Toward that goal, a solution of $Cp(CO)_2RuC(Ph)=C=CH_2$ and $(PPh_3)_2Pt(CO)_2$ in toluene, obtained by reaction of **2** with CO, was treated with an excess of TSI. The ensuing reaction afforded a white precipitate, shown by $^{31}P\{^1H\}$-NMR spectroscopy (δ 5.10, $J_{PtP} = 3698$ Hz) to be a mononuclear platinum phosphine species. One of the two complexes remaining in solution was characterized by ^1H-NMR spectroscopy as unreacted $Cp(CO)_2RuC(Ph)=C=CH_2$, while the other displayed singlet resonances at δ 5.00 (Cp) and 3.16 (CH_2). The position of the δ 3.16 signal is consistent with the complex being a [3 + 2] cycloaddition product of $Cp(CO)_2RuC(Ph)=C=CH_2$ and TSI of structure analogous to that depicted in Eq. (5) [16,25b]. An orange solid isolated upon subsequent addition of pentane showed a FAB mass spectrum appropriate for a $Cp(CO)_2Ru(C_3H_2Ph)$ complex, but with a different fragmentation pattern than that for $Cp(CO)_2RuCH_2C{\equiv}CPh$ [16]. There was no evidence for a 1:1 adduct of $Cp(CO)_2RuC(Ph)=C=CH_2$ and TSI in the spectrum, possibly owing to a facile loss of TSI by the parent molecular ion.

4. Conclusions

This study has shown that the complexes $(PPh_3)_2Pt(\mu\text{-}\eta^1{:}\eta^2_{\alpha,\beta}\text{-}C(R)=C=CH_2)Ru(CO)Cp$ (**1**, **2**) and their PPh_3-replacement derivatives react with both nucleophilic and electrophilic reagents. Reactions of **1** and **2** with nucleophiles are limited to monosubstitution or disubstitution at the Pt center and were observed with PEt_3, $Ph_2PCH_2CH_2CH_2PPh_2$ and *t*-BuNC. Reactions with electrophiles occur with preservation of the Pt–Ru bond or with fragmentation into mononuclear metal products. Thus, reactions of $L_2Pt(\mu\text{-}\eta^1{:}\eta^2_{\alpha,\beta}\text{-}C(R)=C=CH_2)Ru(CO)Cp$ with *p*-$TolS(O)_2NCO$ result in the formation of [3 + 2] cycloaddition and/or addition-hydrogen transfer products $L_2Pt(\mu\text{-}\eta^1{:}\eta^2\text{-}C=C(R)NS(O)_2Tol\text{-}p)C(O)CH_2)Ru(CO)Cp$ and $(PPh_3)_2Pt(\mu\text{-}\eta^1{:}\eta^2_{\alpha,\beta}\text{-}C(R)=C=CHC(O)NHS(O)_2Tol\text{-}p)Ru(CO)Cp$, respectively. In contrast, the reactions of **1** and **2** with *trans*-NCCH=CHCN, $MeO_2CC{\equiv}CCO_2Me$ and $MeO_2\text{-}CC{\equiv}CMe$ (L) afford $Cp(CO)_2RuC(R)=C=CH_2$ and $(PPh_3)_2PtL$. The phenyl-substituted alkynes react similarly, and for $PhC{\equiv}CPh$ the reaction was also shown to proceed in the reverse direction. The overall chemistry of these heterobimetallic complexes is very different from that of the homobimetallic complexes $(CO)_3M(\mu\text{-}PPh_2)(\mu\text{-}\eta^1{:}\eta^2_{\alpha,\beta}\text{-}C(R)=C=CH_2)M(CO)_3$ (M = Fe or Ru), which is dominated by nucleophilic addition reactions [6–9].

5. Supplementary material

Crystallographic data for the structural analyses has been deposited with the Cambridge Crystallographic Data Centre, CCDC no. 135123 for compound $\mathbf{7}\cdot C_3H_6O$ and no. 135151 for compound **10**. Copies of this information may be obtained free of charge from The Director, CCDC, 12 Union Road, Cambridge, CB2 1EZ, UK (Fax: +44-1223-336033; e-mail: deposit@ccdc.cam.ac.uk or http://www.ccdc.cam.ac.uk).

Acknowledgements

We acknowledge financial support of this investigation by the National Science Foundation (NSF), The Ohio State University, and MURST (Rome). Mass spectra were obtained at The Ohio State University Chemical Instrument Center (funded in part by NSF Grant 79-10019). We thank Johnson Matthey Aesar/Alfa for a loan of ruthenium chloride.

References

[1] A. Wojcicki, C.E. Shuchart, Coord. Chem. Rev. 65 (1990) 219.
[2] A. Wojcicki, J. Clust. Chem. 4 (1993) 59.
[3] S. Doherty, J.F. Corrigan, A.J. Carty, E. Sappa, Adv. Organomet. Chem. 37 (1995) 39.
[4] (a) S.M. Breckenridge, N.J. Taylor, A.J. Carty, Organometallics 10 (1991) 837. (b) N. Carleton, J.F. Corrigan, S. Doherty, R. Pixner, Y. Sun, N.J. Taylor, A.J. Carty, Organometallics 13 (1994) 4179.
[5] P. Blenkiron, J.F. Corrigan, N.J. Taylor, A.J. Carty, S. Doherty, M.R.J. Elsegood, W. Clegg, Organometallics 16 (1997) 297.
[6] (a) S. Doherty, M.R.J. Elsegood, W. Clegg, D. Mampe, N.H. Rees, Organometallics 15 (1996) 5302. (b) S. Doherty, M.R.J. Elsegood, W. Clegg, M.F. Ward, M. Waugh, Organometallics 16 (1997) 4251. (c) S. Doherty, M. Waugh, T.H. Scanlan, M.R.J. Elsegood, W. Clegg, Organometallics 18 (1999) 679.
[7] (a) S. Doherty, M.R.J. Elsegood, W. Clegg, M. Waugh, Organometallics 15 (1996) 2688. (b) S. Doherty, G. Hogarth, M.R.J. Elsegood, W. Clegg, N.H. Rees, M. Waugh, Organometallics 17 (1998) 3331.
[8] S. Doherty, M.R.J. Elsegood, W. Clegg, D. Mampe, Organometallics 16 (1997) 1186.
[9] (a) S. Doherty, M.R.J. Elsegood, W. Clegg, N.H. Rees, T.H. Scanlan, M. Waugh, Organometallics 16 (1997) 3221. (b) S. Doherty, G. Hogarth, M. Waugh, T.H. Scanlan, W. Clegg, M.R.J. Elsegood, Organometallics 18 (1999) 3178.
[10] R.R. Willis, M. Calligaris, P. Faleschini, A. Wojcicki, J. Cluster Sci. (in press).
[11] D.F. Shriver, M.A. Drezdzon, The Manipulation of Air-Sensitive Compounds, 2nd ed., Wiley, New York, 1986.
[12] D.D. Perrin, W.L.F. Armarego, D.R. Perrin, Purification of Laboratory Chemicals, Pergamon, Oxford, 1966.
[13] G. Kresze, A. Maschke, R. Albrecht, K. Bederke, H. Patschke, H. Smalla, A. Trede, Agnew. Chem. Int. Ed. Engl. 6 (1967) 149.
[14] R.A. Head, Inorg. Synth. 28 (1990) 132.
[15] Y. Koie, S. Shinoda, Y. Saito, J. Chem. Soc. Dalton Trans. (1981) 1082.

[16] C.E. Shuchart, R.R. Willis, A. Wojcicki, J. Organomet. Chem. 424 (1992) 185.
[17] R.R. Willis, C.E. Shuchart, A. Wojcicki, A.L. Rheingold, B.S. Haggerty (manuscript in preparation).
[18] B.A. Frenz and Associates, Inc., Structure Determination Package, Enraf–Nonius, Delft, Holland, 1985.
[19] G.M. Sheldrick, SHELXL 97, Program for the Refinement of Crystal Structures, University of Göttingen, Germany, 1997.
[20] TEXSAN, Single Crystal Structure Analysis Software, Version 5.0, Molecular Structure Corp., The Woodlands, TX 77381, 1989.
[21] A.C.T. North, D.C. Phillips, F.S. Mathews, Acta Crystallogr. Sect A 24 (1968) 351.
[22] V. Parthasarathi, P.T. Beurskens, H.J.B. Slot, Acta Crystallogr. Sect A 39 (1983) 860.
[23] International Tables for X-ray Crystallography, Kynoch Press, Birmingham, Vol. IV, UK, 1974, pp. 71 and 148.
[24] R.F. Stewart, E.R. Davidson, W.T. Simpson, J. Chem. Phys. 42 (1965) 3175.
[25] (a) W.P. Giering, S. Raghu, M. Rosenblum, A. Cutler, D. Ehntholt, R.W. Fish, J. Am. Chem. Soc. 94 (1972) 8251. (b) S. Raghu, M. Rosenblum, J. Am. Chem. Soc. 95 (1973) 3060. (c) A. Cutler, D. Ehntholt, W.P. Giering, P. Lennon, S. Raghu, A. Rosan, M. Rosenblum, J. Tancrede, D. Wells, J. Am. Chem. Soc. 98 (1976) 3495.
[26] P.B. Bell, A. Wojcicki, Inorg. Chem. 20 (1981) 1585.
[27] J.P. Williams, A. Wojcicki, Inorg. Chem. 16 (1977) 2506.
[28] A.L. Hurley, M.E. Welker, C.S. Day, Organometallics 17 (1998) 2832.
[29] F.P. Pruchnik, Organometallic Chemistry of the Transition Elements, Plenum Press, New York, 1990, Ch. 6.
[30] J. March, Advanced Organic Chemistry, 4th ed., Wiley-Interscience, New York, 1992.
[31] A. Pidcock, in: E.C. Alyea, D.W. Meek (Eds.), Catalytic Aspects of Metal Phosphine Complexes, American Chemical Society, Washington, DC, 1982, p. 1, and references therein.
[32] M.N. Ackermann, R.K. Ajmera, H.E. Barnes, J.C. Gallucci, A. Wojcicki, Organometallics 18 (1999) 787.
[33] (a) M. Rosenblum, Acc. Chem. Res. 7 (1974) 122. (b) A. Wojcicki, in: M. Tsutsui, Y. Ishii, Y. Huang (Eds.), Fundamental Research in Organometallic Chemistry, Van Nostrand-Reinhold, New York, 1982, p. 569. (c) M.E. Welker, Chem. Rev. 92 (1992) 97.
[34] R. Ugo, F. Cariati, G. LaMonica, Inorg. Synth. 11 (1971) 105.
[35] R.-S. Keng, Y.-C. Lin, Organometallics 9 (1990) 289.
[36] P. Blenkiron, S.M. Breckenridge, N.J. Taylor, A.J. Carty, M.A. Pellinghelli, A. Tiripicchio, E. Sappa, J. Organomet. Chem. 506 (1996) 229.